Event-based Green Scheduling of Radiant Systems in Buildings

(Technical Report)

Truong X. Nghiem, George J. Pappas and Rahul Mangharam
Department of Electrical and Systems Engineering
University of Pennsylvania
{nghiem, pappasg, rahulm}@seas.upenn.edu

***Abstract*—This paper looks at the problem of peak power demand reduction for intermittent operation of radiant systems in buildings. Uncoordinated operation of the circulation pumps of a multi-zone hydronic radiant system can cause temporally correlated electricity demand surges when multiple pumps are activated simultaneously. Under a demand-based electricity pricing policy, this uncoordinated behavior can result in high electricity costs and expensive system operation. We have previously presented Green Scheduling with the periodic scheduling approach for reducing the peak power demand of electric radiant heating systems while maintaining indoor thermal comfort. This paper develops an event-based state feedback scheduling strategy that, unlike periodic scheduling, directly takes into account the disturbances and is thus more suitable for building systems. The effectiveness of the new strategy is demonstrated through simulation in MATLAB.**

I. INTRODUCTION

Radiant heating and cooling systems, or radiant systems for short, serve as an alternative to the conventional forced-air heating, ventilating and air conditioning (HVAC) systems for buildings. In radiant systems, heat is supplied to or removed from building elements such as floors, ceilings and walls by circulating water, air or electric current through a circuit embedded in or attached to the structure [1]. Radiant systems depend largely on radiant heat transfer between the thermally controlled building elements and the conditioned space, hence their name.

The benefits of radiant systems over forced-air HVAC systems for residential and commercial buildings have been well-studied [2], [3]. Essentially, there are three major benefits: human comfort, reduced heat loss, and peak energy demand reduction. Because the building elements used in radiant systems have high thermal mass, they serve as energy storage whose slow thermal behaviour is exploited to provide cooling or heating. Hence, the building's thermal mass can be utilized to flatten out peaks in energy demand. Nowadays, radiant systems are widely used in both commercial and residential buildings in Korea, Germany, Austria, Denmark and in some parts of the United States [4].

Two-position control is the simplest type of control for radiant systems, in which the system is switched on or off when the zone temperature reaches certain thresholds. Outdoor reset control, which sets the supply water temperature according to the ambient air temperature by a predetermined rule, and PID control are also used in practice [1]. More advanced control methods have been proposed to control radiant systems to achieve better performance, in particular model predictive control (MPC) was shown to improve the comfort and the energy consumption of radiant systems in [5], [6].

Recently, intermittent operation of the circulation pumps in hydronic radiant systems was investigated in [7] for reducing the electricity consumption of radiant systems. The focus of [7] was on maintaining the thermal comfort in a single zone by achieving good temperature regulation. However, intermittent operation of radiant systems can cause highly fluctuating electricity demand of the pumps, which results in high peaks in the electricity demand. Particularly, in a system of multiple zones with multiple pumps, temporally correlated spikes in the electricity demand can occur when multiple circulation pumps are activated simultaneously. High peaks in electricity demand are costly under a demand-based electricity pricing policy, in which a customer is charged for both its electricity consumption as well as its peak demand over the billing cycle. The unit price of the peak demand charge is usually very high to discourage the use of electricity under peak load conditions. Many commercial electricity customers are subject to demand-based pricing [8]. Therefore reducing the peak electricity demand of intermittent operation of radiant systems is desirable.

In our recent paper [9], the *Green Scheduling* approach was proposed to schedule the operation of electric radiant heating systems to reduce the aggregate peak power demand while ensuring that indoor thermal comfort is always maintained. We studied and applied periodic scheduling, which was simple and scalable but did not take into account disturbances (which are often abundant in building systems). *The major contribution of this paper is the development of an event-based state feedback scheduling strategy, which directly handles the disturbances and is therefore more appropriate for radiant systems in buildings*. Through simulation in MATLAB of a 10-zone hydronic radiant system, our approach was shown to achieve a 77.8% reduction in peak demand and a 31.2% reduction in total energy consumption, compared to uncoordinated operation of the pumps.

This paper is organized as follows. We present the system's model and define the Green Scheduling problem for intermittent operation of circulation pumps of hydronic radiant systems in Section II. The new scheduling algorithm is developed in Sections III and IV. Its effectiveness in reducing peak electricity demand will be demonstrated through MATLAB simulations in Section V. We discuss related work in Section VI. Finally, Section VII concludes the paper with a summary and future research directions.

This material is based upon work supported by the DoE Energy Efficient Buildings (EEB) HUB sponsored by the U.S. Department of Energy under Award Number DE-EE0004261.

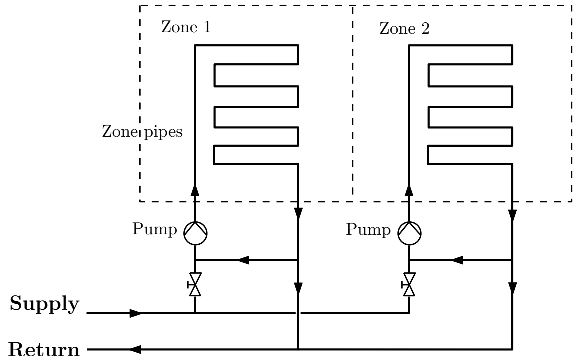

Fig. 1: Diagram of a hydronic radiant system for two zones.

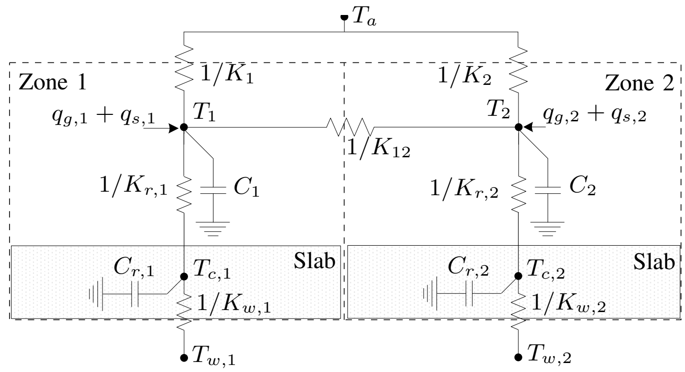

Fig. 2: RC network model of a hydronic radiant system for two zones.

II. System's Model and Problem Definition

Modern radiant systems use either electrical resistance elements (*electric radiant systems*) or fluid flowing in pipes (*hydronic radiant systems*) to heat or cool the building elements [10], [1]. In hydronic radiant systems, hot or chilled supply water is pumped through a system of tubes laid in a pattern inside the radiant building elements. Consider two zones equipped with a hydronic radiant system as depicted in Fig. 1. Embedded in a slab under the floor or above the ceiling of each zone is a piping system that carries water from a supply source, e.g., a boiler system for heating or a chiller system for cooling. The radiant piping systems for the zones are separate, meaning that their water distribution pipes are separate from each other. As illustrated in Fig. 1, each zone has its own supply and return pipes as well as a circulation pump. This hydronic circuit topology is similar to that used in [7] and is one of the topologies proposed in [11]. We first discuss the intermittent operation of circulation pumps in Section II-A. A thermal model for the hydronic radiant system will be described in Section II-B and the Green Scheduling problem will be defined in Section II-C.

A. Intermittent Operation of Radiant Systems

For a hydronic radiant system as in Fig. 1, the supply water temperature and the mass flow rate (by the pump) are the two manipulatable variables for low level control. The water temperature can be regulated by using mixing valves, while the mass flow rate can be changed by variable speed control of the circulation pump. In practice, typically one of these two controllable variables is fixed, or only changed infrequently, and the other is manipulated. That is, either the supply water temperature is fixed and variable speed control is used for the pump, or the pump runs at constant speed and the supply water temperature is varied. However, both options require continuous operation of the circulation pump, which can result in high electricity cost of the radiant system.

Intermittent operation of the circulation pump was studied in [7] for reducing the energy consumption of radiant systems. Essentially, the supply water temperature is fixed and the pump is either switched off or operated at a constant speed. Because of the high thermal inertia of the radiant systems, this simple control method is appropriate for regulating the zone temperature. Furthermore, as the pump no longer runs continuously, the electricity consumption and cost of the system can be reduced. In this paper, we assume this intermittent control method for the circulation pumps.

TABLE I: List of parameters of the RC network model in Fig. 2 for a hydronic radiant system, for $i = 1, 2$.

T_a	ambient air temperature (°C)
T_i	air temperature of zone i (°C)
$T_{c,i}$	core temperature of the slab of zone i (°C)
$T_{w,i}$	supply water temperature for zone i (°C)
$q_{g,i}$	internal heat gain of zone i (W/m^2)
$q_{s,i}$	heat gain due to solar radiation of zone i (W/m^2)
K_i	thermal conductance between zone i and outside air (W/(K m^2))
$K_{r,i}$	thermal conductance between core and air temperatures of zone i (W/(K m^2))
$K_{w,i}$	thermal conductance of the piping system of zone i (W/(K m^2))
K_{ij}	thermal conductance between zone i and zone j (W/(K m^2))
C_i	thermal capacitance of zone i (J/K)
$C_{r,i}$	thermal capacitance of the slab of zone i (J/K)

B. Thermal Model for Radiant Systems

In [12], a mathematical model was developed for the thermal dynamics of hydronic radiant systems as in Fig. 1. It is assumed that the slab is uniformly heated and there is no lateral temperature difference or heat transfer. As proposed in [13] and shown in [14], the 3-dimensional heat transfer model in the slab can be reduced to a 1-dimensional model by establishing a correlation between supply water temperature, core temperature (i.e., mean slab temperature in the plane of the piping system) and zone air temperature. For each zone, the thermal dynamics from the supply water temperature to the zone temperature is then modeled using a Resistance–Capacitance (RC) network model as shown in Fig. 2. The model for each zone i, $i = 1, 2$, has 4 nodes: T_a is the common ambient air temperature, T_i is the zone temperature, $T_{c,i}$ is the core temperature, and $T_{w,i}$ is the supply water temperature. The parameters and variables of the RC network model are summarized in Table I.

Given the RC network model, we can write the differential equations for the dynamic thermal model of the zones and their radiant systems. When the pump of zone i is circulating water in its piping system, the first-order differential equation for the core temperature node $T_{c,i}$ is:

$$C_{r,i} \frac{\mathrm{d}T_{c,i}}{\mathrm{d}t} = K_{r,i}(T_i - T_{c,i}) + K_{w,i}(T_{w,i} - T_{c,i}) \quad (1)$$

When the pump is not running, equivalently the supply water temperature node $T_{w,i}$ is removed, the differential equation for $T_{c,i}$ becomes:

$$C_{r,i} \frac{\mathrm{d}T_{c,i}}{\mathrm{d}t} = K_{r,i}(T_i - T_{c,i}). \tag{2}$$

The first-order differential equation for the zone air temperature node T_i can be written as:

$$\begin{aligned} C_i \frac{\mathrm{d}T_i}{\mathrm{d}t} &= K_{r,i}(T_{c,i} - T_i) + K_i(T_a - T_i) \\ &\quad + \textstyle\sum_{j \neq i} K_{ij}(T_j - T_i) + q_{g,i} + q_{s,i}. \end{aligned} \tag{3}$$

The model for each zone i has two state variables T_i and $T_{c,i}$. It also has three disturbance variables T_a, $q_{g,i}$ and $q_{s,i}$. The supply water temperature $T_{w,i}$ can be regulated or fixed, depending on the control method for the radiant system. Note that the parameters K_{ij}, $i \neq j$, model the thermal interaction, i.e., heat transfer, between adjacent zones.

Let us consider $n > 1$ zones instead of two zones and suppose that $T_{w,i}$ are constant for all i. Define the state vector $x = [T_1, T_{c,1}, \ldots, T_n, T_{c,n}]^T \in \mathcal{X} = \mathbb{R}^{2n}$ and the disturbance vector $d = [q_{g,1}, q_{s,1}, \ldots, q_{g,n}, q_{s,n}, T_a]^T \in \mathbb{R}^{2n+1}$. Let binary variable $u_i \in \{0, 1\}$ denote the status of the pump of zone i: $u_i = 1$ if the pump is running and $u_i = 0$ otherwise. Define the binary vector $u = [u_1, \ldots, u_n] \in \{0, 1\}^n$. Then the differential equations (1) to (3) for all zones can be combined to give a state-space model:

$$\begin{aligned} \dot{x}(t) &= (A_0 + \textstyle\sum_{i=1}^n A_i u_i(t))x(t) + Bu(t) + Wd(t) \\ &= A(u(t))x(t) + Bu(t) + Wd(t) \end{aligned} \tag{4}$$

where $A(u) = A_0 + \sum_{i=1}^n A_i u_i$. We note that:

- The state matrix $A(u)$ of the model depends on u (i.e., switching state matrix) because the differential equation of the core temperature $T_{c,i}$ changes with respect to the pump's status u_i (Eqs. (1) and (2)).
- From the thermal Eqs. (1) to (3), it is evident that the state matrix $A(u)$ is always strictly diagonally dominant with negative diagonal entries, hence it is Hurwitz [15].

C. Green Scheduling for Peak Demand Reduction

As mentioned in Section I, one benefit of radiant systems is their capability to flatten out peaks in energy demand. However, intermittent operation of the circulation pump makes its electricity demand fluctuate significantly when it is switched on and off. Therefore, the peak demand reduction benefit of radiant systems is neutralized for a single zone. Furthermore, in a system of multiple zones, temporally correlated spikes in the energy demand of the radiant system can occur when multiple circulation pumps are activated simultaneously. This phenomenon will be demonstrated in the simulation in Section V, particularly in Fig. 9.

As we discussed in Section I, high peaks in electricity demand can be costly for commercial electricity customers. Therefore, it is desirable to reduce the peak aggregated electricity demand of the pumps. Because the pumps are only switched on and off, reduction of peak electricity demand must be achieved through coordination of the pumps' operations. At the same time, thermal comfort must be maintained in all the zones, specifically the zone temperature T_i should be kept within a comfortable range $[l_i, h_i]$ where $l_i < h_i$ are given. In our previous work [16], [9], we proposed Green Scheduling as an approach for reducing peak energy demand. Essentially, in Green Scheduling, *multiple interacting control systems are coordinated within a constrained peak demand envelope while ensuring that safety and operational conditions are facilitated*. The peak demand envelope is formulated as a constraint on the number of binary control inputs that can be activated simultaneously, that is $\sum_{i=1}^n u_i(t) \leq k \; \forall t \geq 0$ for some given $k \in \{0, 1, \ldots, n\}$. Evidently, this approach can be applied to coordinate the intermittent operations of the pumps. We can now state the Green Scheduling problem for reducing peak electricity demand of the circulation pumps.

Problem 1: Given model (4) of the radiant system, comfort regions $[l_i, h_i]$ for $i = 1, \ldots, n$, and peak constraint $0 \leq k \leq n$, schedule the operations of the circulation pumps so that the peak demand constraint is satisfied at all time while thermal comfort in each zone is maintained.

A control signal $u(\cdot)$ can be thought of as a schedule that switches on-off and coordinates the individual sub-systems. Hence, we will use interchangeably the terms *control signal* and *schedule*, and the terms *controller* and *scheduler*.

III. State Feedback Green Scheduling

Periodic scheduling was utilized in our previous work [16], [9] for Green Scheduling. While being simple and scalable, periodic scheduling does not take into account the influence of disturbances nor feedback information from the plant, hence it is unsuitable when large disturbances are present. In this section, we will develop a state feedback Green Scheduling strategy that can handle large disturbances.

We first define several essential notions of Green Scheduling. Consider the dynamical system with switching state matrix in Eq. (4). Recall that the control inputs u are binary and the state matrix $A(u)$ is Hurwitz for all values of u. In practice, the disturbances d are always bounded. Therefore, we assume that d is constrained in a convex and compact (i.e., closed and bounded) subset $\mathcal{D}$. The peak demand constraint k on the control inputs u is generalized as a non-empty finite constraint set $\mathcal{U} \subseteq \{0, 1\}^n$ of valid control inputs, meaning that $u(t) \in \mathcal{U}$ for all $t \geq 0$. When u is constrained by k, $\mathcal{U} := \{u \in \{0, 1\}^n : \|u\|_1 \leq k\}$.

A disturbance signal $d(\cdot)$ is *admissible* if it satisfies $d(t) \in \mathcal{D}$ for all $t \geq 0$. Similarly, an admissible control signal $u(\cdot)$ satisfies $u(t) \in \mathcal{U} \; \forall t \geq 0$. Given an admissible disturbance signal $d(\cdot)$ and an admissible control signal $u(\cdot)$, a state trajectory $x(\cdot)$ of the system is a continuous signal that satisfies the differential equation (4) at all time. For any initial state $x(0) \in \mathbb{R}^n$, the state trajectory $x(\cdot)$ exists and is unique [17].

Because we are only interested in the zone temperatures T_i, let us define the output vector $y = [T_1, \ldots, T_n]^T$. Obviously $y = Cx$ with an appropriate output matrix $C \in \mathbb{R}^{n \times 2n}$. Let $\mathtt{Safe} \subset \mathbb{R}^n$ denote a compact set of safe, or desired, outputs of the system. For the radiant system in Section II, $\mathtt{Safe}$ specifies the desired zone temperature ranges: $\mathtt{Safe} := [l_1, h_1] \times \cdots \times [l_n, h_n]$. The goal of Green Scheduling is to devise a scheduling strategy for the system so that from any initial state $x(0)$, the output trajectory $y(\cdot)$ is always driven to $\texttt{Safe}$ in finite time and is maintained inside $\texttt{Safe}$ indefinitely, regardless of the (admissible) disturbances. Such an output trajectory is said to be *(eventually always) safe* and is formally defined below.

Definition 1: An output trajectory $y(\cdot)$ is (eventually always) safe if there exists a finite time $0 \leq \tau < +\infty$ such that $y(t) \in \texttt{Safe}$ for all $t \geq \tau$.

A. State Feedback Scheduling Strategy

A state feedback scheduling strategy is a feedback law $\kappa : \mathcal{X} \to \mathcal{U}$ that maps state x to an admissible control input $\kappa(x) \in \mathcal{U}$. The resulting state trajectory $x(\cdot)$ satisfies the *closed-loop* differential equation $\dot{x}(t) = A(\kappa(x(t)))x(t) + B\kappa(x(t)) + Wd(t)$, $\forall t \geq 0$, with initial state $x(0)$. To solve Problem 1, we aim to find a feedback law $\kappa(\cdot)$ such that from any initial state $x(0)$ and for any admissible disturbance signal $d(\cdot)$, the resulting output trajectory $y(\cdot)$ is safe. Such a feedback law is called a *safe state feedback law* (or *safe state feedback scheduling strategy*). To this end, we use the concept of *attracting sets* of control systems [18]. However, to satisfy the finite-time requirement in Definition 1, we modify the definition of attracting sets as follows.

Definition 2: A set $\mathcal{A} \subset \mathcal{X}$ is a (finite-time) attracting set of control system (4) and a set $\mathcal{B} \subseteq \mathcal{X}$ is a basin (or domain) of attraction of $\mathcal{A}$ if there exists an admissible feedback control law $\kappa : \mathcal{X} \to \mathcal{U}$ such that for any initial state $x(0) \in \mathcal{B}$ and any admissible disturbance signal $d(\cdot)$, the resulting state trajectory $x(\cdot)$ satisfies $x(t) \in \mathcal{A}$, $\forall t \geq \tau$ for some finite $\tau \geq 0$.

It is readily seen that if an attracting set $\mathcal{A}$ satisfies $C\mathcal{A} = \{Cx : x \in \mathcal{A}\} \subseteq \texttt{Safe}$ then there exists a safe state feedback scheduling strategy for all $x(0) \in \mathcal{B}$. The following result allows us to determine an attracting set of control system (4) and an associated safe feedback law.

Theorem 1: Let $x_c \in \mathcal{X}$ be a given point in the state space. Suppose there exist $M \in \mathbb{R}^{2n\times 2n}$, $\lambda > 0$ and $\alpha > 0$ such that

$$M \succeq C^T C, \qquad M \succ 0, \tag{5a}$$

$$A(u)^T M + MA(u) \preceq -2\lambda M \qquad \forall u \in \mathcal{U}, \tag{5b}$$

$$\alpha > \frac{1}{\lambda} \max_{z^T M z = 1} \min_{u\in\mathcal{U}} \max_{d\in\mathcal{D}} z^T M(A_0 x_c + \hat{B}u + Wd) \tag{5c}$$

where $\hat{B} = [b_1 + A_1 x_c, \ldots, b_n + A_n x_c]$ and b_i is the i^{th} column of B. Then $\mathcal{A} := \{x \in \mathbb{R}^n : (x - x_c)^T M (x - x_c) \leq \alpha^2\}$ is an attracting set of control system (4) with basin $\mathcal{B} = \mathcal{X}$ and with state feedback law $\kappa(\cdot)$ given by

$$\kappa(x) = \arg\min_{u\in\mathcal{U}} (x - x_c)^T M\hat{B}u, \qquad \forall x \in \mathcal{X}. \tag{6}$$

In addition, if the ball $\mathfrak{B}(Cx_c, \alpha) = \{y : \|y - Cx_c\|_2 \leq \alpha\}$ is a subset of $\texttt{Safe}$ then $\kappa(\cdot)$ is a safe state feedback law.

Due to the page limit, the proof of Theorem 1 is omitted. It is similar to the proof of Theorem 3 in [19] and is given in details in [20]. We make two remarks on this result.

Remark 1: The function $V(x) := (x - x_c)^T M (x - x_c)$ is a robust control Lyapunov function of the control system [21]. Condition (5c) essentially means that for any x outside $\mathcal{A}$, i.e., $V(x) > \alpha^2$, $u = \kappa(x) \in \mathcal{U}$ is such that, for all $d \in \mathcal{D}$, V always decays along the system's flow at a rate not slower than $-\gamma$, for some constant $\gamma > 0$. A detailed argument can be found in [20].

Remark 2: M and λ satisfying conditions (5a) and (5b) can be computed by solving a Generalized Eigenvalue Problem (GEVP) [22], e.g., using the function `gevp` of the Robust Control Toolbox of MATLAB [23].

Theorem 1 immediately gives us a safe feedback scheduling strategy. Note that we only need to re-compute u when x is outside $\mathcal{A}$. Once x is inside $\mathcal{A}$, we can simply keep the current control vector u until x hits the boundary of $\mathcal{A}$. Therefore, a basic feedback scheduling strategy is given by

$$u(t) = \begin{cases} \arg\min_{u\in\mathcal{U}} (x(t) - x_c)^T M\hat{B}u & \text{if } V(x(t)) \geq \alpha^2 \\ u(t^-) & \text{otherwise} \end{cases} \tag{7}$$

in which $u(t^-)$ denotes the currently used control vector. We remark that M, x_c and α are pre-computed and fixed, hence the minimization in Eq. (7) is a combinatorial linear program (LP). Using convex optimization theory [24], we can show that this minimization has the same optimal value as its continuous relaxation $\min_{u\in\text{co}(\mathcal{U})} (x(t) - x_c)^T M\hat{B}u$. Furthermore, the optimal value is always attained at an extreme point of the polyhedron $\text{co}(\mathcal{U})$. Therefore the minimization in Eq. (7) can be replaced equivalently by the binary LP $\arg\min_{u\in\text{co}(\mathcal{U}), u\in\{0,1\}^m} (x(t) - x_c)^T M\hat{B}u$, which can be solved efficiently by a Mixed Integer LP solver such as GUROBI [25].

The basic scheduling strategy in Eq. (7) has several limitations:

1) It requires solving the minimization (7) continuously in real time, which is impractical.
2) It usually results in a high-frequency sliding mode control (SMC) signal [26], when u switches rapidly and repeatedly between two control vectors $u' \in \mathcal{U}$ and $u'' \in \mathcal{U}$, causing x to slide along the boundary of two regions of state: one in which u' is optimal and the other in which u'' is optimal. This effect is often undesirable in practice.

IV. Event-based Green Scheduling

To overcome the aforementioned limitations of the basic feedback law, we will develop in this section an event-based scheduling strategy based on the basic strategy.

Consider any x outside $\mathcal{A}$. The feedback law in Eq. (7) essentially finds a control that always reduces $V(x(t))$ at the fastest rate possible. However, it is certainly sufficient to use a control that reduces $V(x(t))$ at a rate not slower than $-\gamma$ (see Remark 1). That is, as long as the currently used control, denoted $u^\star$, satisfies

$$\max_{d\in\mathcal{D}} \dot{V}(x(t)) = \max_{d\in\mathcal{D}} 2(x(t) - x_c)^T M(A(u^\star)x(t) + Bu^\star + Wd) \\ \leq -\gamma \tag{8}$$

then we do not need to compute and switch to a new control. This observation leads to an event-triggered scheme where we only switch the control when it does not satisfy inequality (8) at the current state.

Define the norm $\|x\|_M := \sqrt{x^T M x}$. Let t be the current time and $x^\star = x(t)$ be the current state. Instead of solving

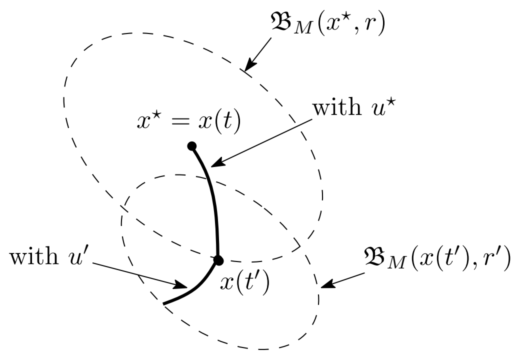

Fig. 3: Illustration of the event-based scheduling strategy.

the optimization (8) continuously in real time, we find a ball $\mathfrak{B}_M(x^\star, r) := \{x : \|x - x^\star\|_M \leq r\}$ with radius $r > 0$ around $x^\star$ so that for all $x \in \mathfrak{B}_M(x^\star, r)$,

$$\max_{d\in\mathcal{D}} 2(x - x_c)^T M(A(u^\star)x + Bu^\star + Wd) \leq -\gamma. \quad (9)$$

Once r is determined, we can keep $u(t') = u^\star$ for $t' \geq t$ as long as $x(t') \in \mathfrak{B}_M(x^\star, r)$ and only compute a new control by Eq. (7) when the event $\|x(t') - x^\star\|_M \geq r$ is detected. This event-triggered scheme is illustrated in Fig. 3. The radius r can be estimated using the following two propositions, whose proofs can be found in the appendix.

Proposition 1: The radius r is bounded below by

$$r_1 = \beta + \tfrac{1}{2}\left(\xi - \sqrt{\xi^2 + 4\beta\xi + \tfrac{4\theta}{\lambda} + \tfrac{2\gamma}{\lambda}}\right) \quad (10)$$

in which $\beta = \|x^\star - x_c\|_M$,

$$\xi = \tfrac{1}{\lambda}\max_{d\in\mathcal{D}} \|A(u^\star)x_c + Bu^\star + Wd\|_M,$$
$$\theta = \max_{d\in\mathcal{D}}(x^\star - x_c)^T M(A(u^\star)x_c + Bu^\star + Wd).$$

Proposition 2: The radius r is bounded below by

$$r_2 = -\frac{\frac{\gamma}{2} + \zeta}{\|(R^{-1})^T A^T M(x^\star - x_c)\|_2 + \chi} \quad (11)$$

in which nonsingular upper-triangular matrix R satisfying $R^T R = M$ is determined by the Cholesky decomposition of M and

$$\chi = \max_{d\in\mathcal{D}} \|A(u^\star)x^\star + Bu^\star + Wd\|_M,$$
$$\zeta = \max_{d\in\mathcal{D}}(x^\star - x_c)^T M(A(u^\star)x^\star + Bu^\star + Wd).$$

Although Eq. (11) has a negation sign, it is usually the case that $\zeta < -\frac{\gamma}{2}$, hence r_2 is usually positive. The radius r is then estimated as the larger value of r_1 and r_2.

Remark 3: Note that in Propositions 1 and 2, M, λ, γ, x_c, $u^\star$, and $x^\star$ are all fixed. Thus the optimization programs involved in those results are simple convex quadratic programs (QP) and LPs, which can be solved efficiently [24].

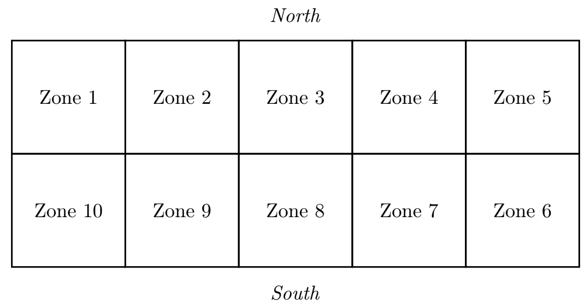

Fig. 4: Layout of the building for the simulation.

A. Improved Scheduling with Disturbance Prediction

If short-term predictions of the disturbances are available, they can be incorporated into the scheduling algorithms to improve Green Scheduling. Specifically, suppose that at any time $t \geq 0$, a prediction of the disturbance constraint set can be obtained for a finite time horizon $h > 0$, that is $d(\tau) \in \mathcal{D}_{[t,t+h]}$ $\forall\tau \in [t, t+h]$, where $\mathcal{D}_{[t,t+h]}$ is known and is not larger than $\mathcal{D}$. Then the event-based scheduling strategy can be modified to exploit this information by replacing $\mathcal{D}$ by $\mathcal{D}_{[t,t+h]}$ in calculations of r_1 and r_2, which often results in larger estimates of r;

V. Simulation Example

We consider a building of 10 zones of equal size as illustrated in Fig. 4. Five of them face north while the other five face south. The building is cooled by a hydronic radiant cooling system with the same configuration as described in Section II and illustrated in Fig. 1. The supply water temperature is the same for all zones and is fixed at a predetermined value T_w.

For each zone, we used the parameter values from [14] for a typical office building, which are summarized in Table II. Because the parameters in [14] are for a single zone, while the considered building has 10 zones, we varied several parameter values for each zone uniformly randomly around the nominal values given in [14]. The range for each of these parameters is also reported in Table II. For the four corner zones 1, 5, 6 and 10 that have two external walls, we increased the thermal conductance K_i accordingly. The comfort range of zone temperature is 22 °C to 26 °C for all zones.

A. Disturbances

The disturbances T_a, $q_{g,i}$ and $q_{s,i}$ affecting each zone are constrained and their time-varying constraint sets are assumed to be known. In particular, weather forecasts give us the ranges of T_a and $q_{s,i}$ for each zone i at any given time during the day. The constraint of $q_{g,i}$ for each zone i can be calculated based on the power rates of the equipment and lights in the zone as well as its occupants' schedules. In this example, we assume the time-varying constraints of T_a, $q_{g,i}$ and $q_{s,i}$, for every $i \in \{1, \ldots, 10\}$, as given in Fig. 5. Note that between the north zones (zones 1 to 5) and the south zones (zones 6 to 10), their solar radiation heat gain profiles are different, as clearly displayed in Fig. 5. Each disturbance signal for each

TABLE II: Parameter values for a zone in the simulation.

Space length, width, height	$6\,\mathrm{m} \times 6\,\mathrm{m} \times 3\,\mathrm{m}$
Façade area	$18\,\mathrm{m}^2$
Internal-wall area	$36\,\mathrm{m}^2$
Thickness of concrete slab	$250\,\mathrm{mm}$
Pipe spacing	$200\,\mathrm{mm}$
External/internal pipe diameter	$20/15\,\mathrm{mm}$
Mass flow rate (per slab area)	$15\,\mathrm{kg/(h\,m^2)}$
$T_{w,i}$	$18\,°\mathrm{C}$
$1/K_i$	[2.1, 2.2] ($\mathrm{K\,m^2/W}$)
$1/K_{r,i}$	[0.124, 0.130] ($\mathrm{K\,m^2/W}$)
$1/K_{w,i}$	[0.05, 0.07] ($\mathrm{K\,m^2/W}$)
$1/K_{ij}$ (only for adjacent zones)	[0.16, 0.20] ($\mathrm{K\,m^2/W}$)
C_i	[1900, 2100] (kJ/K)
$C_{r,i}$	[3000, 4000] (kJ/K)
Desired zone temperature range	[22, 26] (°C)

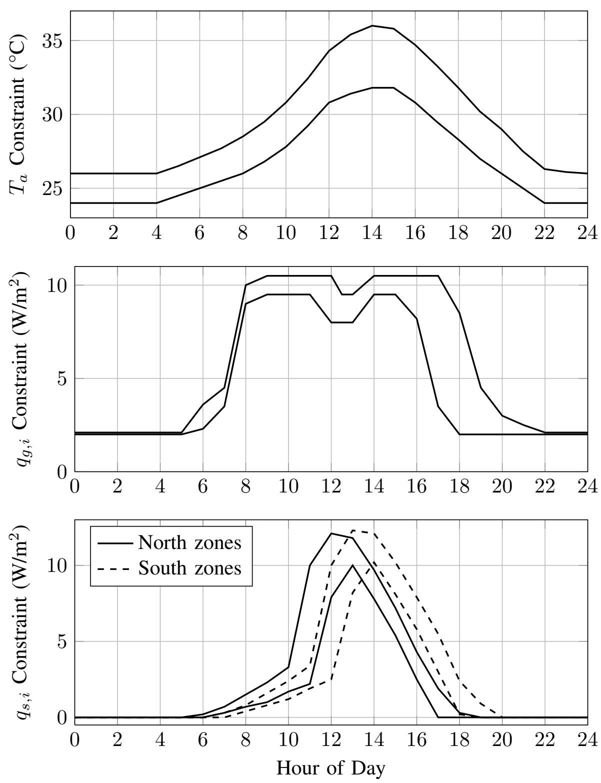

Fig. 5: Time-varying constraints of the disturbances T_a (top), $q_{g,i}$ (middle) and $q_{s,i}$ (bottom) affecting each zone.

zone was then generated uniformly randomly within its given time-varying constraint.

B. Uncoordinated Intermittent Operation

As the baseline control of the radiant system, we considered the uncoordinated intermittent operation of the pumps. For each zone i, its pump is switched on/off independently of the other zones and with hysteresis as follows: whenever zone temperature $T_i \geq 26\,°\mathrm{C}$, $u_i = 1$; whenever $T_i \leq 22\,°\mathrm{C}$, $u_i = 0$. This simple control strategy was simulated in MATLAB for 24 hours (1 day). The initial temperatures for all zones were set to $27\,°\mathrm{C}$. The resulting air temperature T_1 and core temperature $T_{c,1}$ of zone 1 are plotted in Fig. 6.

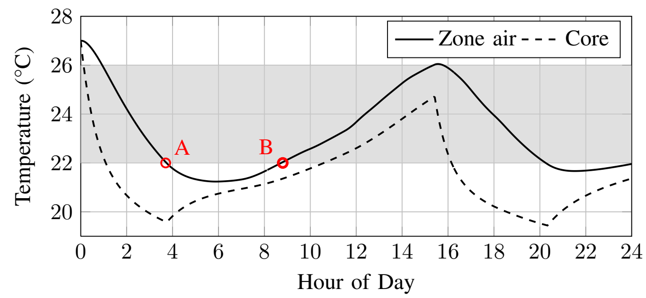

Fig. 6: Air and core temperatures of zone 1 for the unsafe uncoordinated intermittent operation.

As obviously seen in Fig. 6, zone temperature T_1 dropped below $22\,°\mathrm{C}$, to as low as about $21\,°\mathrm{C}$, twice during the day. For example, between points A and B in the figure, T_1 was below $22\,°\mathrm{C}$ for more than 5 hours. This phenomenon can be explained by the high thermal inertia of the radiant system. When the pump was switched off (point A), the slab stopped being cooled; however the core temperature was still significantly below the zone temperature, causing the air to continue being cooled. Therefore T_1 dropped below the lower threshold and only started rising up after several hours.

To avoid this problem, we increased the threshold at which the pump is switched off by $1.15\,°\mathrm{C}$ to $23.15\,°\mathrm{C}$. The new simulation results are reported in Fig. 7. Clearly T_1 was driven to and maintained within the desired range (gray-filled area in the figure).

Because the pumps' power information was not provided in [14], we assumed a normalized power demand of 1 (power unit) for each pump. Figure 9 shows the normalized total power demand of all the pumps (dashed line). Evidently, the demand fluctuated significantly during the day and attained a high peak of 9 during the on-peak hours between 3:30 PM and 5:45 PM. During the off-peak hours before 3:00 AM, a high peak of 10 was attained due to the uncoordinated initialization of the zonal controllers. Thus, under a demand-based electricity tariff, it would incur a high demand cost. The total energy consumption of the pumps was 62.5 (power unit $\times$ hour).

C. Event-based Green Scheduling

To flatten out the high peak demand incurred by the uncoordinated intermittent operation of pumps, the event-based Green Scheduling strategy developed in Section IV was applied. We assumed that at any time, one-hour predictions of the disturbance constraints were available to the scheduler. Therefore, we applied the improved scheduling strategy with disturbance prediction, presented in Section IV-A. The peak constraint on the control inputs was chosen to be $k = 2$ at all time. A MATLAB simulation was performed for 24 hours with the same disturbance profiles and the same initial temperatures as in Section V-B. Figure 8 plots the simulation results for Green Scheduling. It is clear that the temperature of zone 1 (top) was safe as it was driven to and maintained inside the desired range (gray-filled area). Compared to the uncoordinated scheduling, the pump of zone 1 was switched on and off twice as often, however its switching frequency was still slow (less than once every 3 hours). The computation

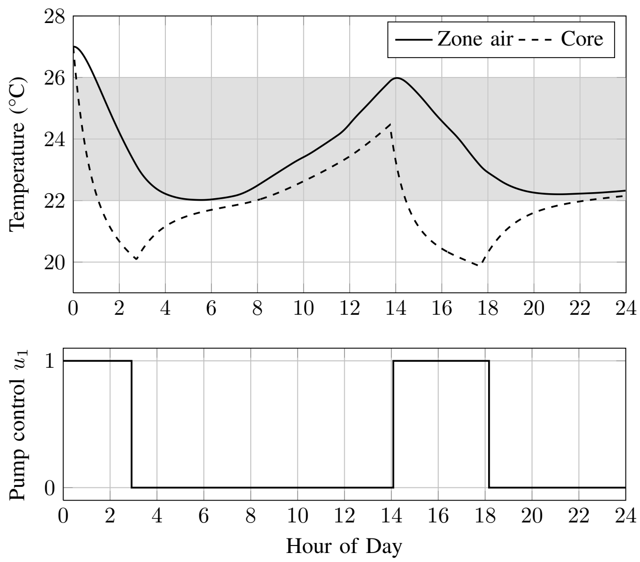

Fig. 7: Temperatures (top) and pump's status (bottom) of zone 1 for the safe uncoordinated intermittent operation.

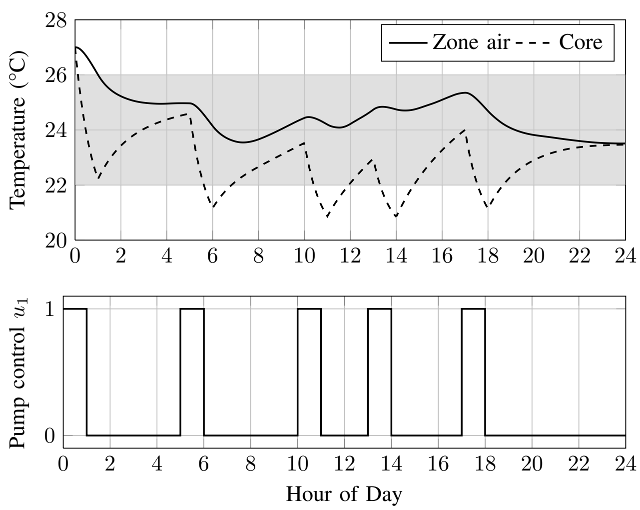

Fig. 8: Temperatures (top) and pump's status (bottom) of zone 1 for the event-based Green Scheduling algorithm with one-hour disturbance predictions.

of each iteration of the event-based scheduling algorithm (i.e., the calculation of radius r) took an average of about $16\,\text{ms}$ on MATLAB on a MacbookPro computer with $2.26\,\text{GHz}$ Core 2 Duo processor and $4\,\text{GB}$ RAM.

The total power demand of the pumps is plotted in Fig. 9 in comparison with that for the uncoordinated intermittent operation in Section V-B. Evidently, the peak demand incurred by Green Scheduling was flattened out and significantly reduced. In fact, the demand of Green Scheduling was constant at 2 for most of the day. The normalized peak demand and total energy consumption of both scheduling strategies are compared in Table III. Note that for the uncoordinated operation, we only report its peak demand during the on-peak hours. By applying Green Scheduling to the radiant system, we saved 77.8% in

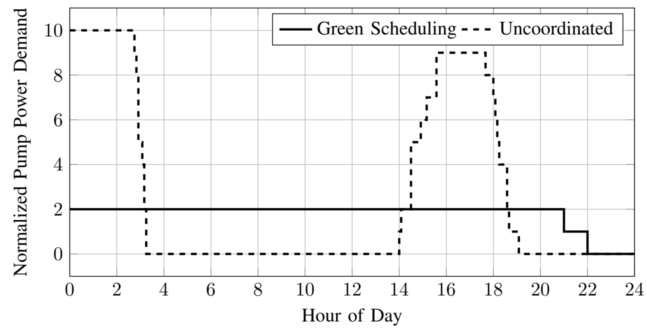

Fig. 9: Normalized total power demand for both scheduling strategies.

TABLE III: Normalized peak demand and total energy consumption of both scheduling strategies.

	Peak	Consumption
Uncoordinated scheduling	9	62.5
Green Scheduling	**2 (-77.8%)**	**43 (-31.2%)**

peak demand and 31.2% in total energy consumption. Under a demand-based electricity tariff, this would amount to a large saving in electricity cost.

VI. Related work

There are various approaches to balance the power consumption in buildings and to flatten out peaks in power demand, e.g., load shifting and load shedding [27]. However, they operate on coarse grained time scales and do not guarantee any thermal comfort. Using a model-based approach, Model Predictive Control (MPC) has received increasing attention in energy efficient control for commercial buildings [28], [29] and in peak electricity demand reduction with real-time pricing [30]. Although MPC can be used for the Green Scheduling problem, the combinatorial nature of the control inputs usually results in mixed integer programs, which can be expensive computationally to solve. Hence we opted for the simple periodic scheduling approach in our previous work [16], [9] and the feedback scheduling approach developed in this paper.

Essentially, the Green Scheduling problem is a safe control problem for switched systems [31]. There has been a vast literature on safe switching controller synthesis for switched systems (e.g., [32], [33], [34]). However, most of these synthesis methods are not scalable in terms of the number of discrete modes and the dimension of the state space, and are thus limited to small-scale systems.

Event-triggering has been used in control theory since the end of the nineties for efficient implementations of control laws in situations where limited resources, such as actuation and network communication, are shared among several subsystems [35], [36], [37]. Similar to this paper, control Lyapunov functions were usually used in the literature for deriving the event-triggering conditions that ensure system's stability or convergence of the system's state.

VII. Conclusion

In this paper, we developed an event-based state feedback scheduling strategy for the Green Scheduling problem, based on the concept of attracting sets of control systems and robust control Lyapunov functions. Unlike the periodic scheduling approach used in our previous work, this new scheduling algorithm uses state feedback and directly takes into account the influence of disturbances. It was applied to scheduling intermittent operations of pumps of hydronic radiant systems. Through simulations in MATLAB, we showed that our approach is effective for reducing the peak electricity demand of the pumps while ensuring that the desired thermal comfort level in each zone is maintained.

For future work, we aim to incorporate continuous control inputs in Green Scheduling. We also want to develop distributed and hierarchical scheduling algorithms for peak demand reduction in extremely large-scale systems. We are also investigating scheduling strategies based on dynamic pricing models that can lead to demand cost reduction in a more on-line fashion.

References

[1] R. Watson and K. Chapman, *Radiant Heating and Cooling Handbook*, ser. McGraw-Hill Handbooks. McGraw-Hill, 2002.

[2] C. Stetiu, "Energy and peak power savings potential of radiant cooling systems in US commercial buildings," *Energy & Buildings*, vol. 30, no. 2, pp. 127–138, 1999.

[3] D. Saelens, W. Parys, and R. Baetens, "Energy and comfort performance of thermally activated building systems including occupant behavior," *Building & Environment*, vol. 46, no. 4, pp. 835–848, 2011.

[4] B. Olesen, "Radiant floor heating in theory and practice," *ASHRAE Journal*, vol. 44, no. 7, pp. 19–24, 2002.

[5] J.-Y. Lee, M.-S. Yeo, and K.-W. Kim, "Predictive control of the radiant floor heating system in apartment buildings," *Journal of Asian Architecture & Building Engineering*, vol. 1, no. 1, pp. 105–112, 2002.

[6] T. Y. Chen, "Application of adaptive predictive control to a floor heating system with a large thermal lag," *Energy and Buildings*, vol. 34, no. 1, pp. 45–51, 2002.

[7] M. Gwerder, J. Tödtli, B. Lehmann, V. Dorer, W. Güntensperger, and F. Renggli, "Control of thermally activated building systems (TABS) in intermittent operation with pulse width modulation," *Applied Energy*, vol. 86, no. 9, pp. 1606–1616, 2009.

[8] M. H. Albadi and E. F. El-Saadany, "Demand response in electricity markets: An overview," in *Proc. IEEE Power Engineering Society General Meeting*, 2007, pp. 1–5.

[9] T. X. Nghiem, M. Behl, G. J. Pappas, and R. Mangharam, "Green scheduling for radiant systems in buildings," in *IEEE Conference on Decision and Control*, 2012.

[10] ASHRAE, *HVAC Systems and Equipment*, ser. ASHRAE Handbook. Atlanta, GA: ASHRAE, 2008.

[11] B. Lehmann, V. Dorer, M. Gwerder, F. Renggli, and J. Tödtli, "Thermally activated building systems (TABS): Energy efficiency as a function of control strategy, hydronic circuit topology and (cold) generation system," *Applied Energy*, vol. 88, no. 1, pp. 180–191, 2011.

[12] M. Koschenz and V. Dorer, "Interaction of an air system with concrete core conditioning," *Energy & Buildings*, vol. 30, no. 2, pp. 139–145, 1999.

[13] J. Seem, *Modeling of heat transfer in buildings*. University of Wisconsin–Madison, 1987.

[14] M. Gwerder, B. Lehmann, J. Tödtli, V. Dorer, and F. Renggli, "Control of thermally activated building systems (TABS)," *Applied Energy*, vol. 85, pp. 565–581, 2008.

[15] R. A. Horn and C. R. Johnson, *Matrix analysis*. Cambridge University Press, 1990.

[16] T. X. Nghiem, M. Behl, R. Mangharam, and G. J. Pappas, "Scalable scheduling of building control systems for peak demand reduction," in *Proceedings of the American Control Conference*, 2012.

[17] W. J. Rugh, *Linear System Theory*. Prentice-Hall, 1996.

[18] H. K. Khalil, *Nonlinear systems*. Macmillan New York, 1992.

[19] A. Girard and G. J. Pappas, "Approximate bisimulation relations for constrained linear systems," *Automatica*, vol. 43, no. 8, pp. 1307–1317, 2007.

[20] T. X. Nghiem, "Green scheduling of control systems," Ph.D. dissertation, University of Pennsylvania, 2012.

[21] Z. Artstein, "Stabilization with relaxed controls," *Nonlinear Analysis: Theory, Methods & Applications*, vol. 7, no. 11, pp. 1163–1173, 1983.

[22] S. Boyd, L. E. Ghaoui, E. Feron, and V. Balakrishnan, *Linear matrix inequalities in system and control theory*. SIAM, 1994.

[23] The MathWorks, "Robust control toolbox," 2012.

[24] S. Boyd and L. Vandenberghe, *Convex Optimization*. Cambridge University Press, 2006.

[25] I. Gurobi Optimization, "Gurobi optimizer reference manual," 2012. [Online]. Available: http://www.gurobi.com

[26] C. Edwards and S. Spurgeon, *Sliding Mode Control: Theory And Applications*. Taylor & Francis, 1998.

[27] K. ho Lee and J. E. Braun, "Development of methods for determining demand-limiting setpoint trajectories in buildings using short-term measurements," *Building & Environment*, vol. 43, no. 10, pp. 1755 – 1768, 2008.

[28] Y. Ma, F. Borrelli, B. Hencey, B. Coffey, S. Bengea, and P. Haves, "Model predictive control for the operation of building cooling systems," in *Proc. ACC*, 2010, pp. 5106–5111.

[29] F. Oldewurtel, A. Parisio, C. N. Jones, M. Morari, D. Gyalistras, M. Gwerder, V. Stauch, B. Lehmann, and K. Wirth, "Energy efficient building climate control using stochastic model predictive control and weather predictions," in *Proc. ACC*, 2010, pp. 5100–5105.

[30] F. Oldewurtel, A. Ulbig, A. Parisio, G. Andersson, and M. Morari, "Reducing peak electricity demand in building climate control using real-time pricing and model predictive control," in *Proceedings of the IEEE Conference on Decision and Control*, 2010, pp. 1927–1932.

[31] H. Lin and P. J. Antsaklis, "Stability and stabilizability of switched linear systems: A survey of recent results," *IEEE Trans. Autom. Control*, vol. 54, no. 2, pp. 308–322, 2009.

[32] J. Lygeros, C. Tomlin, and S. Sastry, "Controllers for reachability specifications for hybrid systems," *Automatica*, vol. 35, pp. 349–370, 1999.

[33] E. Asarin, O. Bournez, T. Dang, O. Maler, and A. Pnueli, "Effective synthesis of switching controllers for linear systems," *Proc. IEEE*, vol. 88, no. 7, pp. 1011–1025, 2000.

[34] S. Jha, S. A. Seshia, and A. Tiwari, "Synthesis of optimal switching logic for hybrid systems," in *EMSOFT*, 2011, pp. 107–116.

[35] K. Åström and B. Bernhardsson, "Comparison of periodic and event based sampling for first-order stochastic systems," in *Proceedings of the 14th IFAC World congress*, vol. 11, 1999, pp. 301–306.

[36] P. Tabuada, "Event-triggered real-time scheduling of stabilizing control tasks," *IEEE Trans. Autom. Control*, vol. 52, no. 9, pp. 1680–1685, 2007.

[37] J. Lunze and D. Lehmann, "A state-feedback approach to event-based control," *Automatica*, vol. 46, no. 1, pp. 211–215, 2010.

Appendix

Brief proof of Proposition 1: It follows from Eq. (5b) that the inequality, for all $x \in \mathfrak{B}_M(x^\star, r)$,

$$\begin{aligned} &-\lambda(x - x_c)^T M(x - x_c) + \\ &\max_{d \in \mathcal{D}} (x - x_c)^T M(A(u^\star)x_c + Bu^\star + Wd) \leq -\tfrac{\gamma}{2} \end{aligned} \quad (12)$$

implies (9). Since $\|x - x^\star\|_M \leq r$, $(x - x_c)^T M(x - x_c) \geq (\beta - r)^2$. From the definition of ξ, we have that for all $x \in \mathcal{X}$

$$\begin{aligned}\max_{d\in\mathcal{D}}(x - x^\star)^T M(A(u^\star)x_c + Bu^\star + Wd) &\leq \lambda\xi \|x - x^\star\|_M \\ &\leq \lambda\xi r.\end{aligned}$$

By writing $x - x_c = (x - x^\star) - (x^\star - x_c)$ in Eq. (12) and using the definition of θ and the above inequalities, we can deduce that the inequality $\lambda\xi r \leq \lambda(\beta - r)^2 - \theta - \frac{\gamma}{2}$ implies inequality (12). It is straightforward to verify that r_1 in (10) satisfies the previous inequality, hence it satisfies (9). ■

Brief proof of Proposition 2: The left hand side of (9) can be written as

$$\begin{aligned}&\max_{d\in\mathcal{D}} 2(x - x_c)^T M(A(u^\star)x + Bu^\star + Wd) \\ &\leq -2\lambda(x-x^\star)^T M(x-x^\star)+2(x^\star-x_c)^T MA(u^\star)(x - x^\star) \\ &\quad + 2\max_{d\in\mathcal{D}}(x^\star - x_c)^T M(A(u^\star)x^\star + Bu^\star + Wd) \\ &\quad + 2\max_{d\in\mathcal{D}}(x - x^\star)^T M(A(u^\star)x^\star + Bu^\star + Wd). \qquad (13)\end{aligned}$$

We have that $\lambda(x - x^\star)^T M(x - x^\star) \geq 0$ and $(x^\star - x_c)^T MA(x - x^\star) \leq r \left\|(R^{-1})^T A^T M(x^\star - x_c)\right\|_2$. From the definition of χ, we can bound

$$\max_{d\in\mathcal{D}}(x - x^\star)^T M(A(u^\star)x^\star + Bu^\star + Wd) \leq \chi r.$$

Using these inequalities in (13), it follows that

$$r \left\|(R^{-1})^T A^T M(x^\star - x_c)\right\|_2 + \chi r + \zeta \leq -\frac{\gamma}{2}$$

implies (9), which gives us the estimate r_2 in (11). ■